

# Synthesis and Characterization of Supported Co<sub>2</sub>P Nanoparticles by Grafting of Molecular Clusters into Mesoporous Silica Matrixes<sup>||</sup>

F. Schweyer-Tihay,<sup>†,‡,§</sup> P. Braunstein,<sup>\*,†</sup> C. Estournès,<sup>‡</sup> J. L. Guille,<sup>\*,‡</sup> B. Lebeau,<sup>§</sup> J.-L. Paillaud,<sup>§</sup> M. Richard-Plouet,<sup>‡</sup> and J. Rosé<sup>†</sup>

Laboratoire de Chimie de Coordination, UMR 7513 CNRS, Université Louis Pasteur, 4 rue Blaise Pascal, 67070 Strasbourg Cedex, France, Groupe des Matériaux Inorganiques, Institut de Physique et Chimie des Matériaux, UMR 7504 CNRS, 23 rue du Loess, 67037 Strasbourg Cedex, France, and Laboratoire des Matériaux Minéraux, UPRES-A 7016 CNRS, Ecole Nationale Supérieure de Chimie de Mulhouse, 3 rue Alfred Werner, 68093 Mulhouse, France

Received June 21, 2002. Revised Manuscript Received September 20, 2002

High-quality Co<sub>2</sub>P nanoparticles have been obtained from diphosphine-substituted molecular cobalt clusters anchored into an inorganic matrix. The synthesis was followed stepwise using a wide panel of analytic techniques. The required functionalization of an ordered mesoporous silica matrix of the type SBA-15 was achieved by covalent attachment of the alkoxysilyl-substituted short-bite diphosphine ligand (Ph<sub>2</sub>P)<sub>2</sub>N(CH<sub>2</sub>)<sub>3</sub>Si(OMe)<sub>3</sub>. Anchoring of the cluster [Co<sub>4</sub>(CO)<sub>10</sub>(μ-dppa)] (dppa = (Ph<sub>2</sub>P)<sub>2</sub>NH) led to an organometallic hybrid mesoporous silica whose thermal treatment led to pure nanocrystalline Co<sub>2</sub>P particles. Compared with the particles obtained in a silica xerogel, those synthesized into the SAB-15 matrix were the most regular in spatial repartition, size, and shape.

## 1. Introduction

Nanomaterials bridge the gap between the molecular scale and the solid state, and nanostructured metals, in particular, bimetallic nanoparticles, are attracting considerable interest in view of their new and/or improved properties compared to those of conventional materials.<sup>1</sup> The design of nanomaterials endowed with size-dependent functions is of considerable importance for potential application as chemical catalysts and as magnetic, electronic, or optical materials.<sup>2</sup> The confinement of metallic nanoparticles in the cavities of meso- or nanoporous inorganic matrixes is an attractive way to stabilize highly dispersed particles and to prevent their coalescence into larger, ill-defined aggregates. Furthermore, the host matrix may control the size, the shape, and the dispersion of the guest particles.<sup>3</sup> The sol–gel process is being increasingly applied to the

design of new materials using functional building blocks,<sup>4</sup> and it has already been used to incorporate mono- and bimetallic species into an inorganic matrix.<sup>5</sup> Furthermore, solids with template-based morphology control, such as zeolites and MCM-41, are currently attracting increasing attention as a way to stabilize highly dispersed metal particles endowed with unique properties.<sup>3,6</sup> A challenging development concerns the use of molecular mixed-metal clusters as precursors to microalloy particles that would not be accessible by other, more conventional approaches. Since the nature of the interactions between the metal cluster and the host matrix plays a dramatic role in the quantity of metal incorporated, it appears interesting to graft such clusters into the pores of the matrix<sup>7</sup> by using a bifunctional ligand that would provide a covalent link between the molecular precursor and the host.<sup>8</sup> This ligand must also lead to a stable molecular species with the minimum risk of breaking the metal–ligand inter-

\* To whom correspondence should be addressed. E-mail: braunst@chimie.u-strasbg.fr.

<sup>†</sup> Université Louis Pasteur.

<sup>‡</sup> Institut de Physique et Chimie des Matériaux.

<sup>§</sup> Ecole Nationale Supérieure de Chimie de Mulhouse.

<sup>||</sup> Dedicated to Prof. B. F. G. Johnson for his outstanding contribution to inorganic and organometallic chemistry.

(1) (a) Gonsalves, K. E.; Li, H.; Perez, R.; Santiago, P.; Jose-Yacaman, M. *Coord. Chem. Rev.* **2000**, 206–207, 607. (b) Toshima, N.; Yonezawa, T. *New J. Chem.* **1998**, 1179.

(2) (a) Schmid, G. *Chem. Rev.* **1992**, 92, 1709. (b) Simon, R. *Adv. Mater.* **1998**, 10, 515. (c) Marder, S. R.; Sohn, J. E.; Stucky, G. D. *Materials for Nonlinear Optics*; American Chemical Society, Washington, DC, 1991. (d) Duan, Z.; Hampden-Smith, M. J.; Datye, A.; Nigrey, P. J.; Quintana, C.; Sylwester, A. P. In *Chemical Processes in Inorganic Materials: Metal and Semiconductor Clusters and Colloids*; Materials Research Society: Pittsburgh, PA, 1992; Vol. 272, p 109. (e) *Metal Clusters in Chemistry*; Braunstein, P., Oro, L. A., Raithby, P. R., Eds.; Wiley-VCH: Weinheim, 1999; Vol. 3.

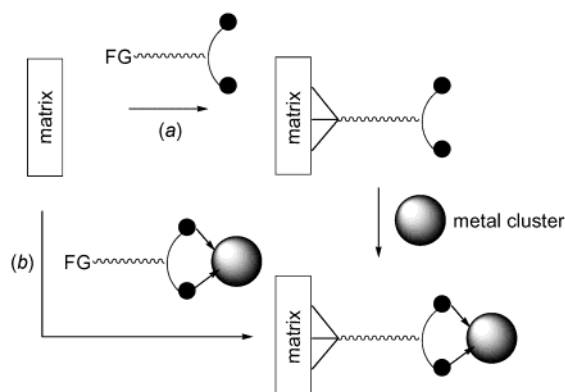
(3) Schweyer, F.; Braunstein, P.; Estournès, C.; Guille, J. L.; Kessler, H.; Paillaud, J.-L.; Rosé, J. *Chem. Commun.* **2000**, 1271.

(4) (a) Corriu, R. J. P.; Leclercq, D. *Angew. Chem., Int. Ed. Engl.* **1996**, 35, 1420. (b) Hüsing, N.; Schubert, U. *Angew. Chem., Int. Ed. Engl.* **1998**, 37, 22. (c) Boury, B.; Corriu, R. J. P. *Chem. Commun.* **2002**, 795.

(5) (a) Shephard, D. S.; Mashmeyer, T.; Johnson, B. F. G.; Thomas, J. M.; Sankar, G.; Ozkaya, D.; Zhou, W.; Oldroyd, R.; Bell, R. G. *Angew. Chem., Int. Ed. Engl.* **1997**, 36, 2242. (b) Braunstein, P.; Cauzzi, D.; Predieri, G.; Tiripicchio, A. *Chem. Commun.* **1995**, 229.

(6) (a) Kresge, C. T.; Leonowicz, M. E.; Roth, W. J.; Vartuli, J. C.; Beck, J. S. *Nature* **1992**, 359, 710. (b) Beck, J. S.; Vartuli, J. C.; Roth, W. J.; Leonowicz, M. E.; Kresge, C. T.; Schmitt, K. D.; Chu, C. T.-W.; Olson, D. H.; Sheppard, E. W.; McCullen, S. B.; Higgins, J. B.; Schlenker, J. L. *J. Am. Chem. Soc.* **1992**, 114, 10834. (c) Corma, A. *Chem. Rev.* **1997**, 97, 2373. (d) Clark, J. H.; Macquarrie, D. J. *Chem. Commun.* **1998**, 853. (e) Ying, J. Y.; Mehnert, C. P.; Wong, M. S. *Angew. Chem., Int. Ed.* **1999**, 38, 56.

(7) (a) Brunel, D.; Bellocq, N.; Sutra, P.; Cauvel, A.; Laspéras, M.; Moreau, P.; Di Renzo, F.; Galarneau, A.; Fajula, F. *Coord. Chem. Rev.* **1998**, 180, 1085. (b) Behringer, K. D.; Blümel, J. *Inorg. Chem.* **1996**, 35, 1814.

**Scheme 1. General Approaches for the Anchoring of Metal Clusters onto Inorganic Matrixes**

action; that is, leaching of the metal should be efficiently avoided. Two general approaches can be envisaged to this aim: attach first one end of the ligand to the inorganic matrix and then react the other functional end with the molecular cluster (Scheme 1a), or first prepare the functionalized cluster and react it with the host matrix to generate the covalent linkage (Scheme 1b).<sup>9</sup>

Thermal treatment of the anchored molecular clusters under appropriate conditions is then expected to lead to nanocomposite products.

The preparation of transition-metal phosphides is generally not easy. They can be synthesized by direct combination of elements at high temperature,<sup>10</sup> by reaction of toxic phosphide with a metal or metal hydride,<sup>11</sup> or by metal organic chemical vapor deposition. Some recent works have developed new routes for synthesizing  $\text{Co}_2\text{P}$  nanocrystals. Xie et al.<sup>12</sup> have prepared nanocrystalline  $\text{Co}_2\text{P}$ ,  $\text{Ni}_2\text{P}$ , and  $\text{Cu}_3\text{P}$  by a direct solvothermal reaction of metal halides with yellow phosphorus, at mild temperatures (80–140 °C), with ethylenediamine as a solvent. They obtained platelike  $\text{Co}_2\text{P}$  particles of about 500-Å diameter, with a wide size distribution. Lukehart and co-workers<sup>8d,13</sup> have synthesized several crystalline nanoclusters of metal phosphide confined into silica xerogels, such as  $\text{Fe}_2\text{P}$ ,  $\text{RuP}$ ,  $\text{Pd}_5\text{P}_2$ ,  $\text{PtP}_2$ ,  $\text{Ni}_2\text{P}$ , and  $\text{Co}_2\text{P}$ , by covalent incorporation into a xerogel of metal complexes containing a bifunctional ligand, with an alkoxysilane function and one or more phosphine groups, followed by thermal treatment under  $\text{H}_2$ . These approaches are very interesting in view of the technological importance of metal phosphides as semiconductors or as phosphorescent, magnetic, or electronic materials.<sup>10a,14</sup>  $\text{Co}_2\text{P}$  has applications in ca-

talysis too, for hydrodenitration.<sup>15</sup> In our study, we have chosen to use mainly an ordered mesoporous silica of the type SBA-15,<sup>16</sup> which is a MCM-41 type material with larger pores (about 90 Å) and walls. To ensure increased molecular stability, the anchoring ligand used was an alkoxysilyl-substituted short-bite diphosphine,  $(\text{Ph}_2\text{P})_2\text{N}(\text{CH}_2)_3\text{Si}(\text{OMe})_3$ ,<sup>9,17</sup> known to strongly bind small transition metal clusters by bridging of a metal–metal bond, thus resulting in the formation of a thermodynamically stable MPNPM' five-membered ring. The molecular cluster to be anchored was chosen as a tetracobalt carbonyl cluster stabilized by bis(diphenylphosphino)amine,  $(\text{Ph}_2\text{P})_2\text{NH}$  (=dppa), which leads to more selective substitution chemistry than the parent  $[\text{Co}_4(\text{CO})_{12}]$ . Furthermore, this red cluster,  $[\text{Co}_4(\text{CO})_{10}(\mu\text{-dppa})]$ , becomes green upon further substitution by a diphosphine, which provides easy evidence for its attachment into the functionalized pores of the host matrix.<sup>9</sup> Thermal treatment performed on these materials led to pure nanocrystalline  $\text{Co}_2\text{P}$  particles that are much better dispersed in the silica hosts than when a silica xerogel, obtained by the sol–gel process, was used.

## 2. Experimental Section

**2.1. Synthesis of the Precursors.** **2.1.1. Synthesis of Ordered Mesoporous Silica SBA-15.**<sup>16</sup> The copolymer triblock poly(ethylene oxide)–poly(propylene oxide)–poly(ethylene oxide) ( $\text{EO}_{30}\text{PO}_{70}\text{EO}_{30}$ ) (Aldrich) (8.0 g) was stirred with 250 mL of  $\text{HCl}$  (1.9 M) for 1 h at 38 °C in a thermostated bath. Then 15.95 mL of  $\text{Si}(\text{OEt})_4$  (TEOS) was added, and the mixture was stirred for 24 h at 38 °C. It was then poured into a bottle and aged for 2 days in a thermostated oven at 90 °C. The solid was filtered and washed with hot chloroform, hot ethanol, and finally with distilled water and then dried at 100 °C under vacuum.

**2.1.2. Synthesis of the Ligand  $(\text{Ph}_2\text{P})_2\text{N}(\text{CH}_2)_3\text{Si}(\text{OMe})_3$  (=dppaSi) (1).**<sup>17</sup> This ligand favors bidentate behavior and thus allows the stabilization of many organometallic clusters.<sup>18</sup> As the reagents are air-sensitive, all the reactions were performed under nitrogen, using standard Schlenk techniques and dried and purified solvents. 3-Aminopropyltrimethoxysilane (5.3 mL, 30.0 mmol) and 9.19 mL (66.0 mmol) of  $\text{NET}_3$  were dissolved in 120 mL of toluene in a two-neck round-bottomed flask. The solution was cooled to –40 °C and 11.14 mL (60.0 mmol) of  $\text{Ph}_2\text{PCl}$  was added dropwise with stirring until room temperature was reached. The mixture was further stirred for 2 h and then filtered. The solvent was removed under reduced pressure and a slightly yellow oil was obtained.

**2.1.3. Synthesis of  $[\text{Co}_4(\text{CO})_{10}(\mu\text{-dppa})]$  (2).**<sup>19</sup> The cluster  $[\text{Co}_4(\text{CO})_{12}]$ <sup>20</sup> was prepared by thermolysis of commercially available  $[\text{Co}_2(\text{CO})_8]$  in hexane. A dichloromethane solution of bis(diphenylphosphino)amine (dppa) was added to  $[\text{Co}_4(\text{CO})_{12}]$  in the ratio 1:1. The resulting cluster (2) is more stable than its precursor.

(8) (a) Mercier, L.; Pinnavaia, T. J. *Adv. Mater.* **1997**, *9*, 500. (b) Brunel, D. *Microporous Mesoporous Mater.* **1999**, *27*, 329. (c) Price, P. M.; Clark, J. H.; Macquarrie, D. J. *J. Chem. Soc., Dalton Trans.* **2000**, 101. (d) Carpenter, J. P.; Lukehart, C. M.; Milne, S. B.; Stock, S. R.; Wittig, J. E.; Jones, B. D.; Glosser, R.; Zhu, J. G. *J. Organomet. Chem.* **1998**, *557*, 121.

(9) Braunstein, P.; Kormann, H.-P.; Meyer-Zaika, W.; Pugin, R.; Schmid, G. *Chem. Eur. J.* **2000**, *24*, 4637.

(10) (a) Aronsson, B.; Lundström, T.; Rundqvist, S. *Borides, Silicides and Phosphides*; Wiley: New York, 1965. (b) Bailar, J. C., Emeleus, H. J., Nyholm, R. S., Troman-Dickenson, A. F., Eds.; *Comprehensive Inorganic Chemistry*, Pergamon Press: Oxford, 1973; Vol. 2. (c) Fruchart, R.; Roger, A.; Senateur, J. P. *J. Appl. Phys.* **1969**, *40*, 1250.

(11) Van Wazer, J. R. *Phosphorus and Its Compounds*, Interscience: New York, 1958; Vol. 1.

(12) Xie, Y.; Su, H. L.; Qian, X. F.; Liu, X. M.; Qian, Y. T. *J. Solid State Chem.* **2000**, *149*, 88.

(13) Carpenter, J. P.; Lukehart, C. M.; Milne, S. B.; Stock, S. R.; Wittig, J. E. *Inorg. Chim. Acta* **1996**, *251*, 151.

(14) (a) Ohta, S.; Onmayashiki, H. *Physica B* **1998**, *253*, 193. (b) Madelung, N. S., Ed. *Landolt-Börnstein*; Springer: Berlin, 1989; Vol. 27a, Group III, p 232. (c) Lukehart, C. M.; Milne, S. B.; Stock, S. R. *Chem. Mater.* **1998**, *10*, 903.

(15) Stinner, C.; Prins, R.; Weber, Th. *J. Catal.* **2001**, *202*, 187.

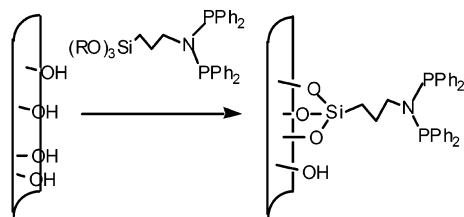
(16) Zhao, D.; Feng, J.; Huo, Q.; Melosh, N.; Fredrickson, G. H.; Chmelka, B. F.; Stucky, G. D. *Science* **1998**, *279*, 548.

(17) Bachert, I.; Braunstein, P.; Hasselbring, R. *New J. Chem.* **1996**, *20*, 993.

(18) Bachert, I.; Braunstein, P.; McCart, M. K.; De Biani, F.; Laschi, F.; Zanella, P.; Kickelbick, G.; Schubert, U. *J. Organomet. Chem.* **1999**, *580*, 257.

(19) Moreno, C.; Macazaga, M. J.; Marcos, M. L.; Gonzalez-Velasco, J.; Delgado, S. *J. Organomet. Chem.* **1993**, *452*, 185.

(20) Chini, P.; Albano, V.; Martinengo, S. *J. Organomet. Chem.* **1969**, *16*, 471.

**Scheme 2. Grafting of 1 into the Pores of SBA-15****Table 1. Porosity Data**

	specific surface area (m <sup>2</sup> /g)	pore diameter (Å)
nongrafted SBA-15	620	90
grafted SBA-15	260	60

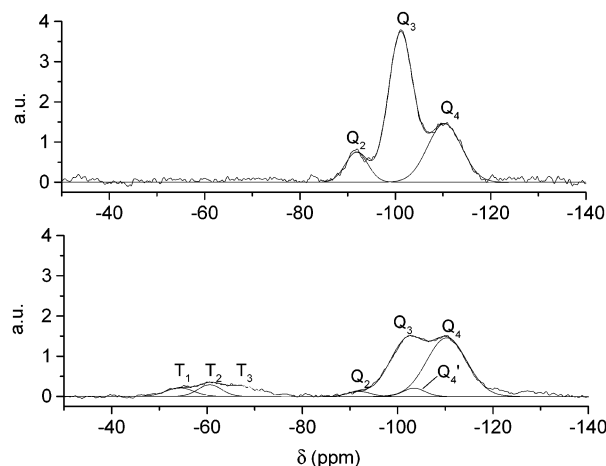
**2.2. Grafting onto the Matrix.** As the phosphine functional groups enhance the rate of condensation of the trialkoxysilyl groups, an *in situ* route was not possible to synthesize functionalized SBA-15 because the silica does not have the time to organize around the template. Post-condensation with the alkoxy silane was then performed (Scheme 2). The dried matrix was soaked in a saturated solution of **1** in THF and then refluxed overnight. The powder was filtered and washed several times to remove the uncondensed alkoxy silane from the pores. It was finally dried under vacuum for 1 night.

**2.3. Anchoring of the Cluster.** The matrix was soaked in a dark red saturated solution of **2** in THF and then refluxed overnight. The resulting powder was filtered and washed several times. Its green color provides evidence for a doubly diphosphine-bridged cluster of the type [Co<sub>4</sub>(CO)<sub>8</sub>(μ-dppa)-(μ-dppaSi)] (Scheme 3).<sup>9</sup>

**2.4. Thermal Treatments.** Since the cobalt atoms in the precursor cluster are already in a low oxidation state, and the degradation of the cluster results in a loss of reductive CO, no additional reducing atmosphere was considered necessary for the thermal treatments. They were performed under argon, at 500 and 800 °C, for 1 h.

**2.5. Characterizations.** **2.5.1. Matrix before Anchoring of the Cluster.** **2.5.1.1. Porosity Measurements.** Specific surface areas have been determined by nitrogen adsorption isotherms on a Sorpt 1750 porosimeter using the BET method. The pore diameter of the nongrafted SBA-15 was imposed by the template used (here 90 Å) and confirmed by TEM observations (Table 1). The pore diameter of the grafted SBA-15 was determined by the BJH method applied on the adsorption branch of the isotherm. X-ray diffraction patterns for both the grafted- and nongrafted SBA-15 show a hexagonal array with a lattice parameter of 101 Å (walls plus pores).

**2.5.1.2. <sup>29</sup>Si NMR Spectroscopy.** The <sup>29</sup>Si MAS and CPMAS NMR measurements were carried out on a MSL 300 spectrometer using a standard 7-mm MAS probe. For MAS NMR, the flip angle was π/6 with a pulse duration of 1.4 μs and a recycle time of 90 s (spinning rate = 4 kHz). For the CPMAS experiment the 90° pulse duration was 4.32 μs, the contact time 5 ms, and the recycle time 10 s (spinning rate 4 kHz). The experiments were performed on a nongrafted matrix and on the SBA-15 grafted by **1**. The NMR technique is useful to

**Figure 1.** <sup>29</sup>Si MAS NMR spectra of SBA-15 before (top) and after grafting of dppaSi (**1**) (bottom).**Table 2. <sup>29</sup>Si NMR Data**

		Q <sub>4</sub>	Q <sub>3</sub>	Q <sub>2</sub>	T
nongrafted	δ (ppm)	-110	-101	-92	
SBA-15	%	59	37	4	
grafted	δ (ppm)	-110	-101	-92	-54 → -67
SBA-15	%	61	29	1	8

determine the degree of hydrolysis and condensation of the network,<sup>21</sup> and thus the relative amount of grafted sites, because the different Si sites have a different chemical shift depending on their degree of condensation.

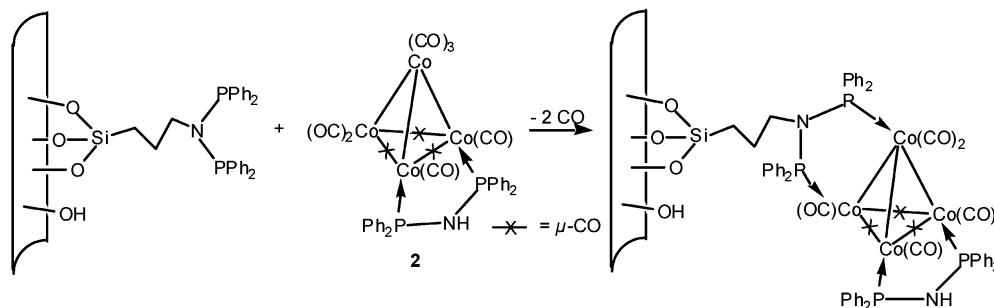
We have determined the contribution of the different silicium sites (Table 2) by appropriate deconvolution of the spectra (Figure 1).

**2.5.1.3. <sup>31</sup>P NMR Spectroscopy.** The <sup>31</sup>P MAS NMR measurements were carried out on a DSX 400 spectrometer using a standard 4-mm MAS probe. The flip angle was π/2 with a pulse duration of 4.6 μs and a recycle time of 120 s (spinning rate = 8 kHz). The experiments were performed on the grafted matrix and the spectra contain peaks around 35 ppm, with their rotational bands (Figure 2).

**2.5.2. Matrix after Anchoring of Cluster 2. Chemical Analysis by Inductively Coupled Plasma (ICP) Analysis.** The Co/Si, P/Si, and Co/P atomic ratios were determined by ICP at the Laboratoire Central d'Analyse de Vernaison (CNRS) and are summarized in Table 3.

According to the stoichiometry of [Co<sub>4</sub>(CO)<sub>8</sub>(μ-dppa)-(μ-dppaSi)], the ratio Co/P should be 1. The result obtained here (0.63) shows that only a fraction (46%) of the anchoring sites has reacted with the precursor cluster.

**2.5.3. Materials after Thermal Treatment.** After thermal treatment at 500 °C, we obtained blue materials that do not present any X-ray diffraction peak except those of the silica matrix. At 800 °C, a black powder was obtained. ICP analysis show a decrease of the amount of P present. Co/P ≈ 1 versus Co/P ≈ 0.63 before calcination.

**Scheme 3. Anchoring of the Cluster 2 in a Derivatized Pore**



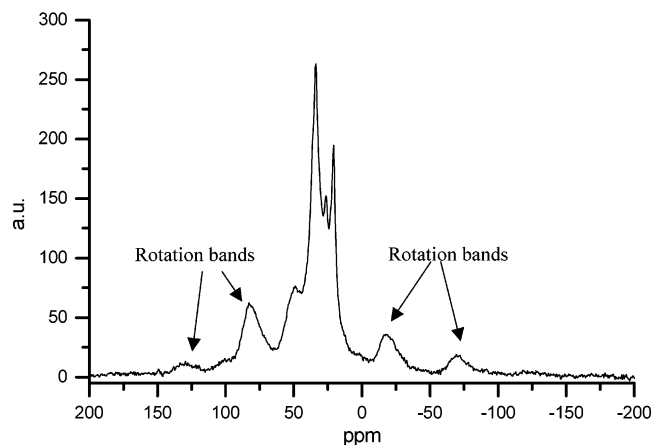


**Figure 2.**  $^{31}\text{P}$  MAS NMR spectra of grafted SBA-15.

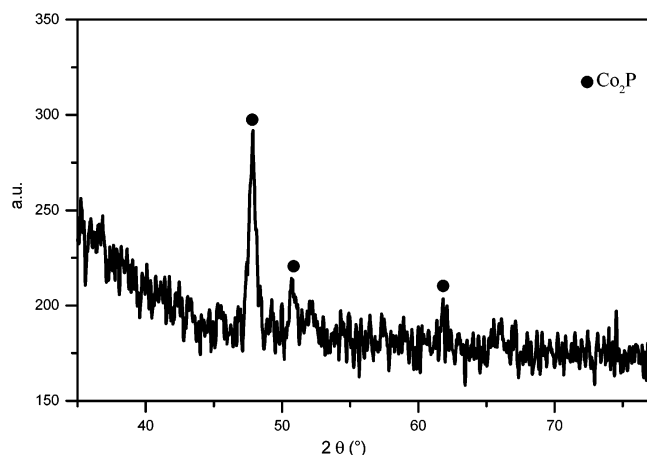


**Figure 3.** X-ray diffraction patterns (cobalt anode) of functionalized SBA-15 grafted with the  $[\text{Co}_4(\text{CO})_{10}(\mu\text{-dppa})]$  cluster and calcined at 800 °C, under argon.

**Table 3. Elemental Analysis of the Samples**

	P/Si	Co/Si	Co/P
SBA-15 before anchoring of <b>2</b>	0.075		
SBA-15 after anchoring of <b>2</b>	0.075	0.05	0.63

**2.5.3.1. X-ray Powder Diffraction.** A Siemens D500 diffractometer equipped with a quartz monochromator and a cobalt anticathode ( $K_{\alpha 1} = 1.78897 \text{ \AA}$ ) working at 35 kV and 30 mA was used on the thermally treated matrix (Figure 3).

Peaks characteristic of  $\text{Co}_2\text{P}$  appeared on the amorphous background. The cell parameters are in good agreement with the reported data:<sup>22</sup> ca.  $a = 5.68(4) \text{ \AA}$ ,  $b = 6.66(3) \text{ \AA}$ , and  $c = 3.48(4) \text{ \AA}$  for the SBA-15 supported nanoparticles.

**2.5.3.2. Transmission Electron Microscopy.** TEM investigations were made using a Topcon 002B electron microscope operating at 200 kV with a point-to-point resolution  $r = 1.8 \text{ \AA}$ . The samples were sonicated in ethanol and deposited on a holey copper grid.

Very regular 60- $\text{\AA}$  nanoparticles, homogeneously distributed, have been observed (Figure 4a). Electron nanodiffractions performed on the particles show the diagram of the orthorhombic  $\text{Co}_2\text{P}$  (Figure 4b). The histogram of the distribution of the particles is shown in Figure 5.

### 3. Results and Discussion

We have succeeded in grafting a bifunctional alkoxy-silyldiphosphine onto an ordered silica matrix and then

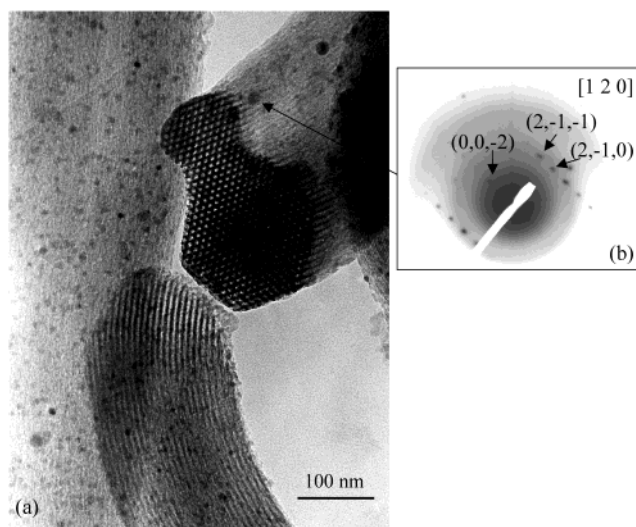


**Figure 4.** (a) TEM micrographs of functionalized SBA-15 anchored with the cluster  $[\text{Co}_4(\text{CO})_{10}(\mu\text{-dppa})]$  (**2**) and treated under argon at 800 °C. (b) Electron nanodiffraction performed on one particle.

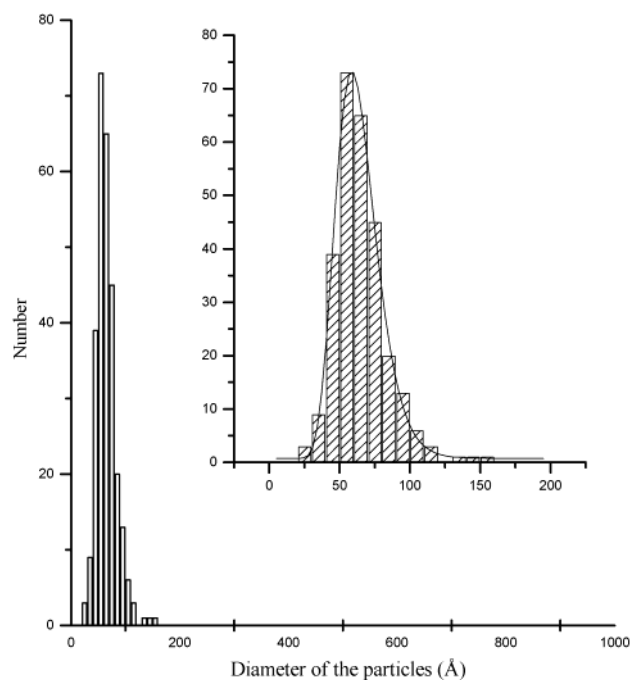


**Figure 5.** Distribution of the diameters of the  $\text{Co}_2\text{P}$  nanoparticles in SBA-15 determined from the analysis of several TEM images (zoom between 0 and 200  $\text{\AA}$ ), with its log-normal fit.

anchor to it a tetracobalt carbonyl cluster. The different characterizations performed allowed us to monitor the evolution of our material, at each step of its synthesis.

**3.1. Before Anchoring of the Cluster 2.** The material still has open pores after grafting of the phosphine linker, with high surface areas (Table 1), which is very interesting for potential catalytic applications. The grafting was rather efficient, with an average P/Si ratio of 0.075 (ICP analysis).

The  $^{29}\text{Si}$  MAS NMR measurements clearly point to the occurrence of the grafting (Figure 1). The appearance of T sites at around -60 ppm and the decrease of the  $\text{Q}_3$  and  $\text{Q}_2$  contributions show that a functional group has been attached onto the matrix. The contribu-

(21) Lindner, E.; Schneller, T.; Auer, F.; Mayer, H. A. *Angew. Chem., Int. Ed.* **1999**, *38*, 2154.

(22) JCPDS Card File 32-306, International Center for Diffraction Data.

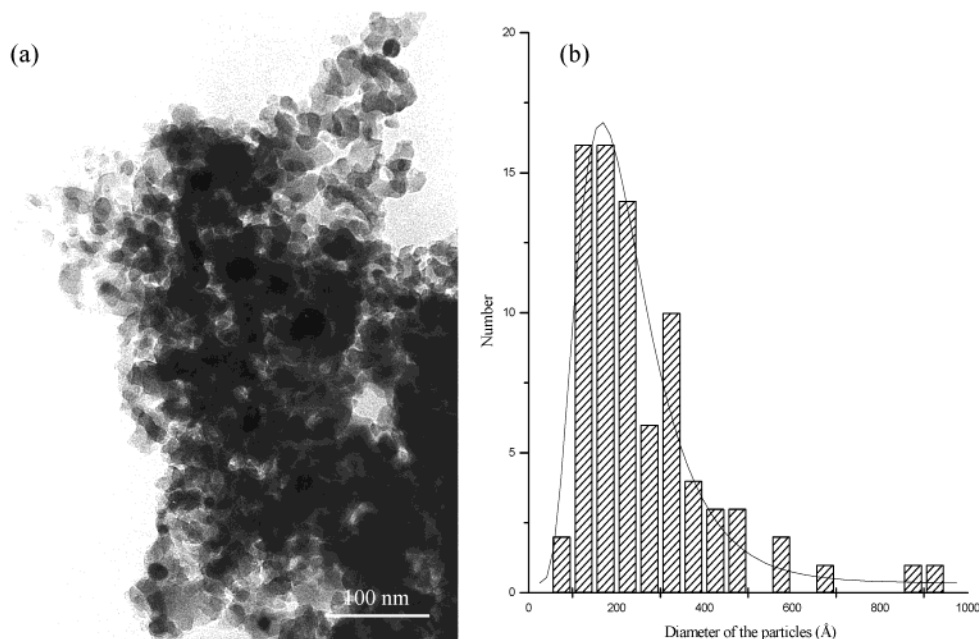


**Figure 6.** (a) TEM micrographs of a functionalized xerogel anchored with the cluster  $[\text{Co}_4(\text{CO})_8(\mu\text{-dppa})]$  (**2**) and treated under argon at 800 °C. (b) Distribution of the diameters of the Co<sub>2</sub>P nanoparticles in the xerogel matrix, with its log-normal fit.

tion of T sites, corresponding to the P/Si ratio, is 8%, consistent with the ICP results (7.5%). If we consider that all the Q<sub>3</sub> and Q<sub>2</sub> are surface silanols, we can evaluate the contribution of pore silanols to be around 40%. With a T site contribution of 8%, we can approximately evaluate the grafting ratio at the surface to be 21%. To obtain a good fit of the spectra, we had to take into account the contribution of Q<sub>4</sub>' sites<sup>23</sup> corresponding to Q<sub>4</sub> sites in direct contact with Q<sub>3</sub> or Q<sub>2</sub> and it was possible to deconvolute the three different contributions of the T<sub>1</sub>, T<sub>2</sub>, and T<sub>3</sub> sites of the grafted SBA-15 (Figure 1, bottom). In CP-MAS, the T sites were even more visible, but the integrations of the peaks are not quantitative.

The <sup>31</sup>P NMR measurements show four peaks at around 45, 35, 15, and 10 ppm. The peak at 35 ppm is attributed to the dppa function, whereas the peaks at 15 and 10 ppm correspond to oxidized dppa.<sup>24</sup> Their deconvolution gives an amount of oxidized phosphine of 30%, and these sites will not be available for the anchoring of the cluster. Whereas a shoulder at 45 ppm remains nonelucidated, the peak at 35 ppm corresponds to dppa and integrates for 50% of the signal. This is consistent with the fraction of cluster-anchored sites determined by ICP to be 46%.

**3.2. After Anchoring of Cluster 2.** The first evidence for the anchoring of cluster **2** in the matrixes is the green color of the materials obtained. Thus, a solution of  $[\text{Co}_4(\text{CO})_{10}(\mu\text{-dppa})]$  has a maximum absorption in UV/vis spectroscopy at around 509 nm, whereas a solution of  $[\text{Co}_4(\text{CO})_8(\mu\text{-dppa})\{\mu\text{-P,P}-(\text{Ph}_2\text{P})_2\text{N}(\text{CH}_2)_3\text{-Si}(\text{OMe})_3\}]$  has its maximum at around 614 nm. The ICP measurements (Table 3) show a Co/Si ratio of about 5%. This ratio of incorporation is higher than when  $[\text{Co}_4(\text{CO})_{12}]$  is just impregnated (around 3%).<sup>25</sup>

Furthermore, the Co/P ratio is 63%; this proves that only a part of the anchoring sites are occupied.

<sup>31</sup>P MAS NMR measurements have been performed on the anchored materials, but no peak was visible, probably owing to some paramagnetic cobalt nuclei<sup>26</sup> from oxidized cluster molecules. <sup>31</sup>P SEM NMR<sup>27</sup> confirmed the presence of some oxidized material.

**3.3. After Thermal Treatment at 800 °C.** The observed increase of the ratio Co/P from 0.63 to 1.0 as determined by ICP indicates that loss of volatile compounds containing phosphorus has occurred. This has already been observed by Lukehart et al.<sup>14c</sup> in the case of dicobalt carbonyls linked to two monophosphines and then grafted onto the pores of silica xerogels. The X-ray diffraction patterns clearly show that Co<sub>2</sub>P has been formed during the thermal treatment. The difference in stoichiometry between the ICP measurements (Co/P = 1) and the composition of the cobalt phosphide (Co/P = 2) indicates that a fraction of the phosphorus is incorporated into the silica matrixes. Using the Scherrer equation, we can estimate the size of the Co<sub>2</sub>P crystallite  $D = K\lambda/\beta \cos \theta$ , where  $K$  is a constant equal to 0.9,  $\lambda$  is the wavelength of the X-ray used,  $\beta$  is the fwhm of the peak, and  $\theta$  the Bragg angle for the peak. We find for  $D$  a value around 60 Å. The TEM observations showed the particles are well-dispersed in each of the host matrixes used. Their average diameter is  $\approx 60$  Å in the SBA-15, which is in good agreement with the size of the crystallite size found by X-ray diffraction; the particles formed are thus single crystals.

(25) Schwyer, F.; Braunstein, P.; Estournès, C.; Guille, J. L.; Kessler, H.; Paillaud, J.-L.; Rosé, J. Unpublished results.

(26) (a) Blumberg, W. E. *Phys. Rev.* **1960**, *119*, 79. (b) Ma Mar, G. N.; Horrocks, W. D.; Holm, R. H. *NMR of Paramagnetic Molecules*; Academic Press: New York, 1973; Chapter 1. (c) Kraus, H.; Prins, R. *J. Catal.* **1997**, *170*, 20.

(27) (a) Tong, Y. Y. *J. Magn. Reson. A* **1996**, *119*, 22. (b) Tuel, A.; Canesson, L.; Volta, J. C. *Colloids Surf., A* **1999**, *158*, 97.

(23) Engelhardt, G.; Michel, D. *High-Resolution Solid-State NMR of Silicates and Zeolites*; John Wiley and Sons: New York, 1987.

(24) Bhattacharyya, P.; Slawin, A. M. Z.; Woollins, J. D. *Inorg. Chem.* **1996**, *35*, 3675.

As one can see from the micrograph (Figure 4) and the histogram (Figure 5), the size and shape of the particles are very regular in the SBA-15 matrix. The diameters of the particles are centered on 60 Å and follow a sharp log-normal distribution (fwhm = 18 Å). Their diameter corresponds to that of the pores, and we therefore suppose that the silica matrix has not been affected by the thermal treatment and the formation of nanoparticles, leading to the size of the nanoparticles being imposed by the diameter of the pores.

For comparison, we have prepared nonordered materials by using grafted xerogels,<sup>28</sup> in which we anchored the cluster.<sup>29</sup> The functionalization has been achieved by an in situ route, with the same phosphine ligand (**1**), leading to a hybrid material, with a P/Si = 0.095, corresponding to the nominal stoichiometry (0.1), a specific surface area of 320 m<sup>2</sup>/g, and a pore diameter centered around 100 Å. This matrix is thus comparable to the grafted SBA-15, only the arrangement and the shape of the pores differ. After anchoring of the cluster **2**, the Co/Si ratio was 0.078, and the ratio Co/P was 0.87, corresponding to a fraction of anchored sites of 87%.

(28) Synthesis of the grafted xerogel: The synthesis was performed under argon. Molar composition: 1:4:0.45:4.5:1:0.05:6 TEOS:EtOH:HNO<sub>3</sub>:H<sub>2</sub>O:HCONH<sub>2</sub>:dppaSi:THF. The phosphine (0.50 g, 1.15 mmol) was diluted in 10 mL of THF (138 mmol); 4.78 g (23 mmol) of TEOS and 4.23 g (92 mmol) of ethanol were added and stirring was maintained for 1 min. In another beaker, 1.86 g (92 mmol) of an aqueous solution of HNO<sub>3</sub> (0.1 M) was mixed with 1.04 g (23 mmol) of formamide and then added to the first solution. Further stirring was maintained for 1 h. Aging in an oven at 40 °C was carried out for 5 days, and the resulting gel was dried under a flux of argon for 2 days and then under vacuum for 24 h. While drying, the gel cracked into small pieces.

(29) Anchoring of the cluster: the xerogel was finely crushed, soaked in a dark red saturated solution of [Co<sub>4</sub>(CO)<sub>10</sub>(μ-dppa)] in THF, and then refluxed overnight. The resulting powder was filtered and washed several times.

Thermal treatment at 800 °C under argon led to 200-Å Co<sub>2</sub>P nanoparticles, but their size and spatial distribution is less regular than that in the organized matrix (Figure 6).

#### 4. Conclusion

The preparation of high-quality Co<sub>2</sub>P nanoparticles confined in a silica matrix has been achieved in the course of this work. The synthesis was followed stepwise using a wide panel of analytic techniques. The synthesis requires a mesoporous silica matrix functionalized by covalent bonding of an alkoxysilyl-substituted short-bite diphosphine (Ph<sub>2</sub>P)<sub>2</sub>N(CH<sub>2</sub>)<sub>3</sub>Si(OMe)<sub>3</sub>. The incorporation of the cluster [Co<sub>4</sub>(CO)<sub>10</sub>(μ-dppa)] led to an organometallic hybrid mesoporous silica. After thermal treatment under argon, pure nanocrystalline Co<sub>2</sub>P particles were obtained. Such particles can also be obtained in silica xerogels by our sol-gel method or by covalent grafting of metal complexes, as reported by Lukehart who obtained ≈50-Å Co<sub>2</sub>P nanoparticles with a fwhm of 40 Å.<sup>8d,13</sup> The decisive influence of the matrix on the size, shape, and distribution of the nanoparticles has to be emphasized and we found that the particles were most regular in repartition, shapes, and size distribution when the SBA-15 matrix is used.

**Acknowledgment.** We are grateful to Luc Delmotte for MAS NMR measurements, to Renée Siegel for assistance with the analysis of the CP MAS NMR spectra, and to Dr. Marc Drillon for valuable discussions. We acknowledge the Ministère de la Recherche, the Centre National de la Recherche Scientifique, and the Région Alsace for support (doctoral grant to F.S.).

CM020132M